MEASUREMENT OF RESIDUAL STRESSES IN ADDITIVE MANUFACUTRED PART

A thesis report submitted in partial fulfillment of the requirements for the degree of

MASTER OF TECHNOLOGY

by

DIGVIJAY CHANDRASEN THAKARE

Roll No: 234103415

Under the supervision of

Prof. SHRIKRISHNA N. JOSHI

DEPARTMENT OF MECHANICAL ENGINEERING
INDIAN INSTITUTE OF TECHNOLOGY GUWAHATI
GUWAHATI- 781039, INDIA

November, 2023

Department of Mechanical Engineering
Indian Institute of Technology Guwahati
Guwahati, India - 781039

CERTIFICATE

This is to certify that the work contained in this thesis titled "**MEASUREMENT OF RESIDUAL STRESSES IN ADDITIVE MANUFACUTRED PART"** by **Mr. DIGVIJAY CHANDRAASEN THAKARE (234103415),** a student of the Department of Mechanical Engineering, Indian Institute of Technology Guwahati, for the award of degree of **Master of Technology** has been carried out under my supervision and that this work has not been submitted elsewhere for any degree.

Prof. Shrikrishna N. Joshi
Professor
Department of Mechanical Engineering
Indian Institute of Technology Guwahati
Guwahati, Assam, India -781039
June 2024

DECLARATION

I declare that this written submission represents my ideas in my own words and where others' ideas or words have been included, I have adequately cited and referenced the sources. I also declare that I have adhered to all principles of academic honesty and integrity and have not misrepresented or fabricated or falsified any idea or data or fact or source in my submission. I understand that any violation of the above will be cause for disciplinary action by the Institute and can also evoke penal action from the sources that have thus not been properly cited or from whom proper permission has not been taken when needed.

Mr. Digvijay Chandrasen Thakare
Roll Number: 234103415
Machine Design (2023-25)
Department of Mechanical Engineering,
IIT Guwahati, Assam, India - 781039

ACKNOWLEDGEMENT

Firstly, I would like to express my sincere gratitude and appreciation to my supervisor, Professor Shrikrishna N. Joshi, Department of Mechanical Engineering, IIT Guwahati, India, for their unwavering guidance, expertise, and continuous encouragement throughout the course of this research. His mentorship has been instrumental in shaping this project.

I am indebted to the dedicated staff and fellow researchers at Department of Mechanical Engineering, IIT Guwahati, India, who provided technical assistance, insightful discussions, and shared their expertise, which significantly contributed to the success of this project.

I extend my heartfelt appreciation to my family members for their unwavering support throughout my master's journey. I am grateful to all the individuals who have inspired me along this journey. Your encouragement and belief in my abilities have been a constant source of motivation. This project would not have been possible without the collective efforts and support of these individuals and organizations. I am truly thankful for their contributions to my academic and research endeavors.

Mr. Digvijay Chandrasen Thakare
Roll Number: 234103415
Machine Design (2023-25)
Department of Mechanical Engineering,
IIT Guwahati, Assam, India - 781039

ABSTRACT

This study aims to investigate the residual stresses induced in additively manufactured AISI 316L stainless steel and Ti 6 Al 4V through Laser Metal Deposition (LMD), a technique widely utilized in high-precision additive manufacturing (AM) applications. Residual stresses play a crucial role in determining the structural integrity, mechanical properties, and durability of AM-produced components. However, they are challenging to manage due to the rapid thermal cycling inherent to the LMD process. These thermal cycles, which occur during the layer-by-layer fabrication of parts, lead to temperature gradients that result in the development of residual stresses within the material. In this research, we analyze the temperature distribution across samples produced by LMD, focusing on how varying thermal profiles contribute to the formation and magnitude of residual stresses. AISI 316L, a stainless-steel alloy and Ti 6 Al 4V known for its excellent corrosion resistance and high-temperature strength, is chosen for its relevance in critical applications where material performance is essential. To accurately measure the induced residual stresses, we employ X-Ray Diffraction (XRD), a reliable and precise method for assessing stress profiles in metallic materials. The study aims to provide insights into the correlation between thermal distributions and residual stress fields, which could inform strategies for process parameter optimization. These findings have significant implications for enhancing the quality, reliability, and longevity of LMD-manufactured components, paving the way for improved performance in industrial applications.

CONTENT

LIST OF FIGURES

CHAPTER 1

CHAPTER 2

CHAPTER 3

CHAPTER5

LIST OF TABLES

CHAPTER 1

CHAPTER 1
INTRODUCTION AND LITERATURE REVIEW

1.1 Additive Manufacturing

1.1.1 Introduction

Additive Manufacturing (AM) has been defined by the ISO/ASTM 52900 committee as: *"process of joining materials to make parts from 3D model data, usually layer upon layer, as opposed to subtractive manufacturing and formative manufacturing methodologies"*.

Rapid Prototyping (RP) techniques, which were first used in the late 1980s and early 1990s as a means of accelerating product development since they could create intricately sculpted prototypes in short amounts of time, gave rise to additive manufacturing processes.

A 3D CAD design model of what we imagine the part to be is the first step in an AM process. After that, this model is broken down into thin slices. The AM machine receives the data and uses it to construct the product layer by layer.

AM procedures construct 3D components by layering material on top of one another, in contrast to traditional subtractive manufacturing methods like machining, which create parts by removing material from a larger piece. This makes it possible to build intricate shapes and geometries and gives designers more creative freedom. These are the main benefits of AM, along with the quick prototyping.

AM is used in various engineering applications like aerospace, bioengineering, automotive sector. The major benefit of using AM is it can be used to produced various parts which might have intrinsic shape and dimension also such parts can be manufactured using various different types of materials.

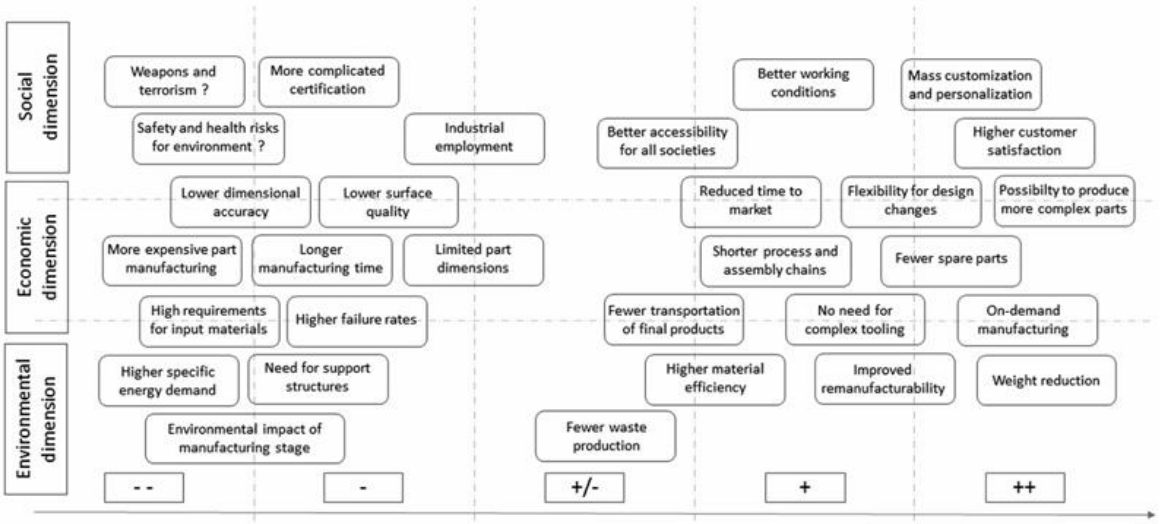

Figure 1.1: Benefits (++) and weaknesses (–) of additive manufacturing processes compared to conventional manufacturing processes.[1]

1.1.2 Types of Additive Manufacturing Process

Seven different processes of Additive Manufacturing have been defined by ISO/ASTM 52900 committee are as follows:

1. **Material extrusion:** The process where material is dispensed through a nozzle or orifice as per need.
2. **Material jetting:** The process where droplets of material is deposited.
3. **Binder jetting:** The process where liquid bonding is used to bind the powder material as per the design.
4. **Sheet lamination:** The process in which material in sheet form is bonded and given the required shape and dimension.
5. **Vat photo-polymerisation:** The process in which liquid photo-polymer in a vat is selectively cured by light-activated polymerisation.
6. **Powder bed fusion:** The process where powder bed is selectively fused using thermal energy or laser.
7. **Directed energy deposition:** The process where focused thermal energy is used to fuse materials by melting as the material is deposited.

1.1.3 Metal Additive Manufacturing

Metal additive manufacturing (MAM) is the term for the additive manufacture of metals. It is a rapidly evolving technology, mostly because it is now considered a manufacturing technique and no longer solely utilized to create prototypes.

The benefits of AM include the ability to quickly prototype and create more intricate structures, as was previously discussed. Additionally, it has been utilized to improve or further develop completed items. Nevertheless, limited production, poor surface quality, and uncertainty about the ultimate mechanical qualities continue to be obstacles.

Among the seven processes mentioned above in 1.1.2, four can be used for metals:

1. **Binder Jetting**
2. **Sheet Metal Lamination**
3. **Powder Bed Fusion**- Selective Laser Sintering (SLS), Selective Laser Melting (SLM), Electron Beam Melting (EBM) and Direct Metal Laser Sintering (DMLS)
4. **Directed Energy Deposition**- Electron Beam Additive Manufacturing (EBAM) and Laser Engineered Net Shaping (LENS), Laser Metal Deposition (LMD)

1.2 Laser Metal Deposition (LMD)

LMD, due to its flexible powder feeding system, is a powerful AM process to build multi-material structure [2]. LMD is a DED technique that uses a laser as its energy source to create near-net-shaped parts layer by layer. It can be utilized for 3D metallic printing. Metal particles are melted and quickly solidified on the surface of a base plate or earlier layers after being introduced into the laser beam via a nozzle during the deposition process. Sometimes post-treatment procedures are needed to enhance the comprehensive characteristics and/or dimensional accuracy. Other well-known names for LMD include direct laser

metal deposition (DLMD), direct laser deposition (DLD), laser engineered net shaping (LENS), and others [3].

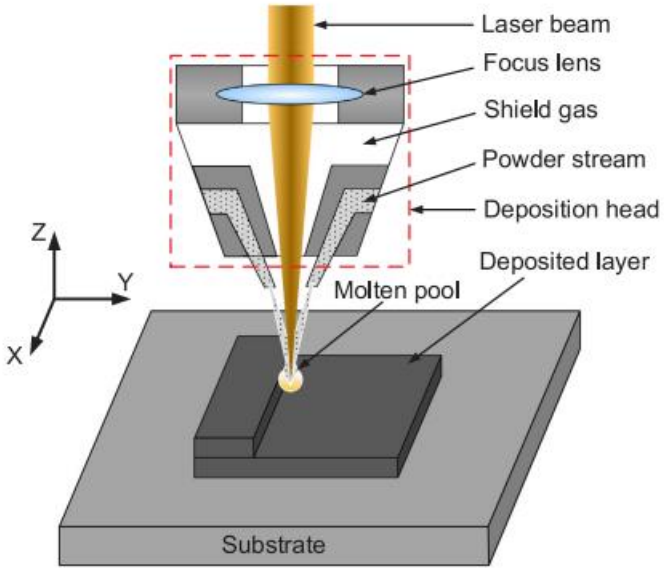

Figure 1.2: Schematic representation of LMD- AM process [4]

Flexible coating, 3D component repair, and additive modification are all accomplished with conventional laser metal deposition. Very big components can also be handled using this technology because it does not require a process chamber. High strength, frequently on par with conventional standards, can be attained by metallurgically bonding the applied layers to the substrate.

A weld pool is produced in traditional laser metal deposition when the workpiece is locally heated by the laser beam. A nozzle in the processing optics sprays fine metal powder straight into the weld pool. There, the fine metal powder melts and joins the base substance. This creates beads that are fused together to create structures on pre-existing basic bodies or whole parts. Numerous layers can be constructed one on top of the other if necessary. On 3D surfaces, laser metal deposition may produce high build or volume rates of many mm^3/sec [6].

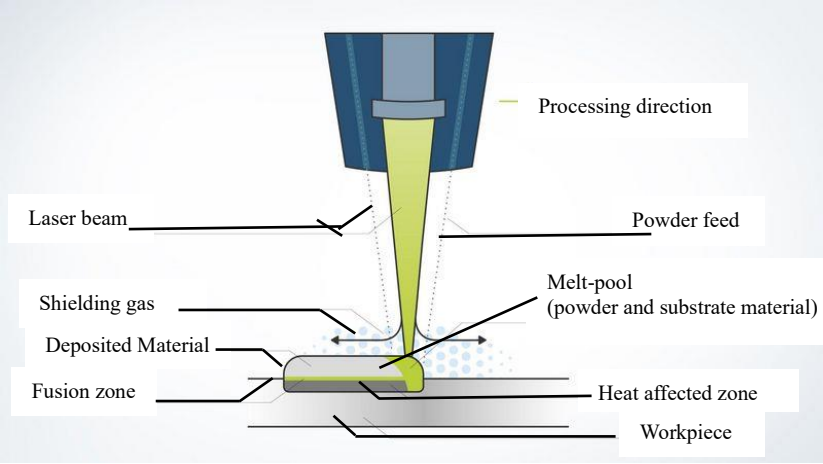

Figure 1.3: Laser Metal Deposition [5]

Larger build volumes are possible with LMD's rapid build pace. A layer thickness of 40 mm to 1 mm can be used to achieve spot size, scan speed, and laser power build rates of up to 300 cm^3/h, depending on the primary parameters [7].

1.3 Laser metal deposition techniques

There are various laser metal deposition techniques where laser is used to supply the energy and nozzle is used to deposit the metal powder on a surface which then solidifies. These processes are used to manufacture and repair parts according to need and feasibility.

1.3.1 Laser powder injection

With this method, powder is injected through a nozzle, melted, and then deposited. Inert gas or a gravity feed can be used to inject the powder. Shielding gas is typically added to the system to stop potential oxidation from forming a pool of molten weld. This method is quite beneficial in that it may be used when adding material to an existing component, particularly for cladding and repairs. But the lack of the method's incapacity to deposit the same quantity of material [9].

1.3.2 Optomec Laser Engineered Net Shaping (LENS)

Sandia National Laboratory initially developed this powder injection technique, which Optomec has been licensed to use for further development and manufacturing. It uses a high power (500W to 4KW) laser as an energy source to deposit metal powder onto a

molten pool of metal, and machines that use it can work with the majority of commercial powders. The technique has a high cooling and solidification rate, but it has a serious overhang problem because the supporting structures are not made of different material [9].

1.3.3 Accufusion Laser Consolidation

The National Research Council of Canada's General Electric (GE) Global Research and Integrated Manufacturing Technologies Institute works together to develop the metal powder injection technique known as laser consolidation. Accufusion has been granted a license to use this method going forward. The procedure is quite similar to the LENS method, which uses a laser to provide the necessary energy to deposit metal powder into a pool of molten metal. A numerical control system regulates the corresponding movement between the laser beam and the substrate. The movement of the laser beam and powder feed nozzle, which creates layer by layer beads of molten material on the substrate that solidify rapidly, is ensured by a predesigned portion from the CAD model. Nevertheless, the technique produces a superior surface polish than the LENS system while having a lower deposition rate [10].

1.4 Light Amplification By The Stimulated Emission Of Radiation

Laser technology is essential to LMD because it allows the metal to transition from a solid to a liquid state, which enables the entire deposition process. Gordon Gould first proposed the idea of a laser, which stands for "Light Amplification by the Stimulated Emission of Radiation," in 1957. He described a method for creating light, or a stimulated emission, using excited atoms or ions [11].

Theodore Maiman demonstrated the first laser in 1960 with his pulsed ruby laser, which employed high electrical voltages to produce a burst of light that excited the ruby crystal's atoms, which in a specific energy state are capable of releasing photons. The idea of gas lasers was first introduced in 1960 as well. This was the helium-neon laser, which, like the ruby laser, stimulated atoms with an electric discharge to produce light.

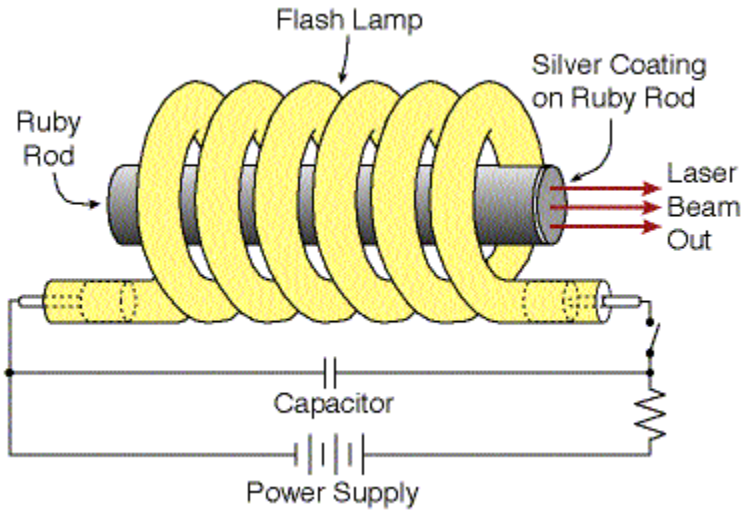

Figure 1.4: Schematic Description of the First Ruby Laser [14]

The same concept, which states that a diode is utilized to generate gain through the flow of electrical current that results in a photon discharge, was also used to present the first diode laser [12].

Similar to the light from a regular lightbulb, laser beams are made up of electromagnetic radiation waves with a specific, consistent wavelength that fall into the visible, ultraviolet, or infrared regions. These waves are coherent light, assuming the same direction and frequency and having a constant phase between them, which makes it possible to predict the electric field of a point through another [12]. Unlike other forms of light waves, laser can propagate through long distances given the high intensity and the fact that the beam is well collimated.

Depending on whether the stimulation is generated in a solid, liquid, or gaseous form, various kinds of lasers can be produced. But the three primary laser types that are most frequently utilized in the majority of industries, which are as follows [15],

- **Semiconductor laser:** The most prevalent type of semiconductor lasers are diode lasers, which generate light by means of electrically or occasionally optically pumped mechanisms.
- **Solid-state laser:** These rely on ion-doped crystals or glasses that are pumped using laser diodes or discharge lamps; the most popular methods for achieving gains are Nd:YAG, Nd:YVO4, and Nd:Glass, among others.
- **Gas laser:** In order to excite the gas, these usually employed electrical discharges (usually CO2, argon, or even gas combinations, such Helium-Neon).

The most common lasers used in LMD are typically from the solid-state laser family, which includes disk, diode, and fiber lasers, among others [16].

1.5 Process parameters for LMD

The following paragraphs go into detail about several crucial process parameters that must be managed in order to achieve the intended results and process aim.

1.5.1 Laser power (P)

The amount of heat source energy that is used for processing materials is known as laser power [17] and it is measured in Watt (W or kW). Control over the laser power is necessary since it significantly affects the process efficiency as well as the mechanical and microstructural characteristics of items made using the LMD technology. The type of material is the most important consideration when choosing the ideal laser power. When too much power is used, the deposited material may dilute and evaporate, and when too little power is used, inappropriate melting may occur, resulting in porosity and subpar layer junctions [17]. The depth, height, and width of the remelted layer grow with increasing laser power, while porosity decreases and it has negative impact on the UTS of material [19].

1.5.2 Scanning speed (V)

Scanning speed is another important parameter as it controls the length of time that the laser, substrate, and deposited material interact. While a low scanning speed can result in dilution and evaporation, a high rate can cause the deposited material to melt improperly. It is important to note that laser power and laser scanning speed are inversely related [17].

$$E\ (J/mm^2) = P/dV \quad \text{.....(1.1)}$$

E= Laser Energy (J/mm^2)

P= Laser Power (W)

V= Scanning speed (m/s)

d= laser beam or spot diameter

1.5.3 Laser beam diameter

The laser beam diameter is measured at the perpendicular focal distance and is expressed in millimeters (mm). The laser spot size (beam diameter) has a crucial impact on the width of deposited layers and has an inverse relation in the LMD process. The laser beam diameter also affects the layer thickness and part quality [17].

1.5.4 Powder feeding rate

One important factor that affects how much material is supplied from the nozzle at any given time is the powder feeding rate. It has a significant effect on the amount of powder used as well as the mechanical, chemical, density, and metallurgical characteristics of the final product [17].

1.5.5 Laser standoff distance

The distance between the laser source and the deposition surface is known as the laser standoff distance. Laser standoff distance affects a number of critical parameters, including heat input, bead geometry, cooling rate, and process stability [20].

1.5.6 Layer thickness or height step

The height step, also known as layer thickness, is the separation in the height direction between two successive layers. Although it is usually maintained constant, the layer thickness might vary depending on the conditions of the operation. Density and cooling may be reduced as the number of cladding layers increases. Although layer thickness measurement can take a lot of time, it is an important factor to take into account during the LMD process since it influences the final components' overall mechanical and metallurgical characteristics [17].

1.6 Feedstock for AM

Metals like Al alloys, steel, Ti and its alloys, Ni Alloys, CoCr are commonly used for additive manufacturing. These metals are converted in powder form for LMD process.

1.6.1 Powder Production

Methods such as water, gas or plasma atomization are used to produce the powder form of metals. For Ti and Ti alloys, metallothermic processes (e.g. TIRO process) and the hydride-dehydride process are used due to its cost-effective metal powder production.

1.6.2 Plasma atomization

Similar to gas atomization, plasma atomization uses a plasma torch to atomize the molten material into droplets rather than a high-pressure gas. A smaller particle size distribution and better flowability are the results of the plasma torch's increased energy input to the atomization process.

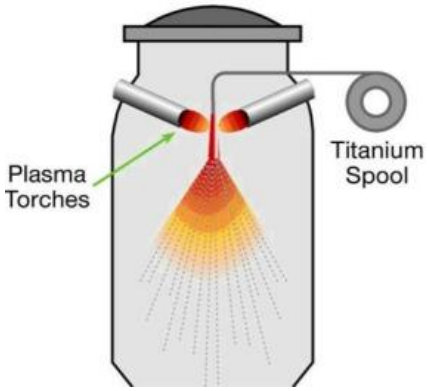

Fig 1.5: Plasma atomization process [21]

The technique of plasma atomization (PA) turns raw materials with a high melting point into high-quality, highly spherical particles. A plasma torch melts the feedstock, which is wire, once it is fed into a chamber. Within the chamber, the melt atomizes concurrently in an inert gas environment with low vacuum. When the metal droplets fall freely into the chamber, they solidify. Since the atomized droplets never come into contact with any solid surface during solidification, this method also reduces the material's possible contaminants.

The majority of the particles produced fall between 0 and 106 μm, with the particle size distribution extending from 0 to 250 μm [17].

1.7 Material and material properties

Additive manufacturing is one of the newest powder metallurgy techniques and as mentioned in 1.5, Al alloys and Ti alloys are widely used. For AM, the fundamental physical and mechanical properties provide reference for the properties of additive manufactured part.

1.7.1 Ti-6Al-4V

The table 1.1 and table 1.2 lists the fundamental physical and mechanical properties of the Ti-6Al-4V respectively.

Physical property	**Value**
Density of solid (ρ)	4.43 g/cm^3
Density of liquid (ρ)	3.89 g/cm^3
Solidus temperature	1877 K (1604°C)
Liqudus temperature	1933 K (1660°C)
Temperature of (α+β) →→ β	1253K (980°C)
Temperature of α →→ β	~1023K (750°C)
Thermal conductivity of solid (k_s)	6.7 W/m/K
Thermal conductivity of liquid (k_l)	32.5 W/m/K
Specific heat capacity of solid (Cp_s)	0.526 J/g/K
Specific heat capacity of liquid (Cp_l)	0.872 J/g/K
Coefficient of thermal expansion of solid (K^{-1})	8.6 μm/m/K
Temperature of martensite phase transformation (M_s)	~1053K (780°C) or ~883K(610°C)

Table 1.1: Fundamental physical properties of Ti-6Al-4V [17]

Mechanical property	Value
Tensile strength, yield ($\sigma_{0.2}$)	880 MPa
Tensile strength, Ultimate (UTS)	950 MPa
Elongation (ε)	14 %
Reduction of Area (R)	36%
Hardness, Hv	349
Young's modulus (E)	113.8 GPa
Poisson's ratio (υ)	0.342
Fracture toughness	75 MPa•$m^{1/2}$

Table 1.2: Mechanical properties of Ti-6Al-4V [17]

1.7.2 SS 316

Physical property	Value
Density of solid (ρ)	8 g/cm^3
Density of liquid (ρ)	7 g/cm^3
Solidus temperature	1648 K (1375°C)
Liqudus temperature	1673 K (1400°C)
Thermal conductivity of solid (k_s)	16.2 W/m/K
Thermal conductivity of liquid (k_l)	30 W/m/K
Specific heat capacity of solid (Cp_s)	0.5 J/g/K
Specific heat capacity of liquid (Cp_l)	0.8 J/g/K
Coefficient of thermal expansion of solid (K^{-1})	16.5 µm/m/K

Table 1.3: Fundamental physical properties of SS 316 [22]

Mechanical property	Value
Tensile strength, yield ($\sigma_{0.2}$)	240 MPa
Tensile strength, Ultimate (UTS)	515 MPa
Elongation (ε)	40 %
Reduction of Area (R)	60%
Hardness, Hv	165
Young's modulus (E)	193 GPa
Poisson's ratio (υ)	0.27
Fracture toughness	80 MPa• $m^{1/2}$

Table 1.4: Mechanical properties of SS 316 [22]

CHAPTER 2
Literature Survey

2.1 Residual stress

Shu-guang Chen[23] delves into the critical aspect of how varying laser power settings impact the microstructure and mechanical properties of 316L stainless steel produced using Laser Metal Deposition (LMD). Through meticulous analysis, the researchers observed that different laser power levels resulted in significant variations in grain structure and phase composition. Specifically, higher laser power tended to produce larger grain sizes and altered phase distributions, which play a crucial role in determining the material's mechanical behavior. Additionally, the study found that mechanical properties such as tensile strength, hardness, and ductility were significantly influenced by the laser power. By fine-tuning the laser power settings, the researchers were able to enhance these properties, leading to improved performance and reliability of the deposited material. This optimization is crucial for practical applications where mechanical integrity is paramount. Moreover, the paper highlighted the influence of laser power on the material's porosity and the presence of microstructural defects. These defects, which are inevitable to some extent in additive manufacturing processes, were found to be significantly affected by the laser power. Higher laser power generally led to reduced porosity and fewer defects, contributing to the overall mechanical robustness of the material. The findings of this research are particularly relevant for industries that rely on additive manufacturing techniques, such as aerospace, automotive, and medical sectors. By providing insights into the optimal laser parameters, this study offers valuable guidance for achieving desired material characteristics, ensuring both efficiency and quality in manufacturing processes. [23].

2.1.1 Formation of residual stress

The paper titled "In situ investigation of phase transformations in Ti-6Al-4V under additive manufacturing conditions combining laser melting and high-speed micro-X-ray diffraction" Kenel, C. [24] published in Scientific Reports focuses on the phase

transformations in Ti-6Al-4V alloy during additive manufacturing. The researchers used a combination of in situ X-ray diffraction and high-speed imaging to monitor the phase evolution in real-time under rapid laser heating and cooling conditions. They observed the $\beta \rightarrow \alpha'$ bi phase transformation and estimated the martensite start temperature to be 923 K. The study provides valuable insights into the phase transformations and microstructural changes that occur during the additive manufacturing process, which is crucial for optimizing the properties of Ti-6Al-4V components used in industries such as aerospace, medical, and automotive [24].

Firstly, is the temperature gradient mechanism. A molten pool forms when the material is quickly heated to the melting point while being exposed to the heat source's radiation. When heated, the material expands and exerts an expansion force outside the molten pool boundary, which tends to cause the component to bulge upward. However, because of the temperature differential, the expansion is constrained by the surrounding material and the boundary. A portion of the thermal strain is converted to plastic strain because metal yields very easily at high temperatures. A temperature gradient of up to 10^4 K/mm forms close to the molten pool as the heat source moves, quickly cooling and solidifying the formerly molten pool at a rate of between 10^3 and 10^7 K/s [23][24]. During cooling and solidification, the materials around the molten pool limit its shrinkage. Furthermore, additional strain is required to compensate during the cooling process of the molten pool because some of the thermal strain is converted into plastic strain during the heating process. A high magnitude tensile residual stress is created close to the molten pool as a result of this strain compensation and the material's mechanical characteristics, which progressively improve as the temperature drops. The cool-down phase mechanism is the second mechanism. Layer-by-layer manufacturing is AM's most notable characteristic. In this procedure, the lower layer that was deposited first limits the shrinkage of the subsequently deposited layer as it cools. As a result, the most recent layer to be deposited experiences tensile tension, and the previously deposited layer experiences additional compressive stress. In order to balance the tensile tension dispersed close to the surface, compressive stress will continue to build up inside the sample as it is deposited layer by layer [23].

The paper titled "Heat Source Modeling and Residual Stress Analysis for Metal Directed Energy Deposition Additive Manufacturing", Kiran, A. [25] published in MDPI's Materials journal, focuses on developing a streamlined heat source model for Directed Energy Deposition. The researchers compared the new concentrated heat source model with the well-established Goldak heat source model. They discovered that the new model required less preprocessing time and computational resources while still accurately predicting the melt pool shape and temperature distribution. The study highlighted the importance of precise heat source modeling in understanding the thermal dynamics of the deposition process. By accurately modeling the heat source, the researchers were able to better predict the evolution of thermal stresses during the DED process. This is crucial because residual stresses can significantly affect the mechanical performance and structural integrity of the manufactured components. The findings underscore the critical role that efficient and accurate heat source models play in the additive manufacturing process. The concentrated heat source model offers a promising alternative for engineers and researchers aiming to optimize manufacturing parameters and improve the quality of DED-produced parts. This advancement could lead to more efficient and reliable production techniques in various industries, including aerospace, automotive, and biomedical engineering [25].

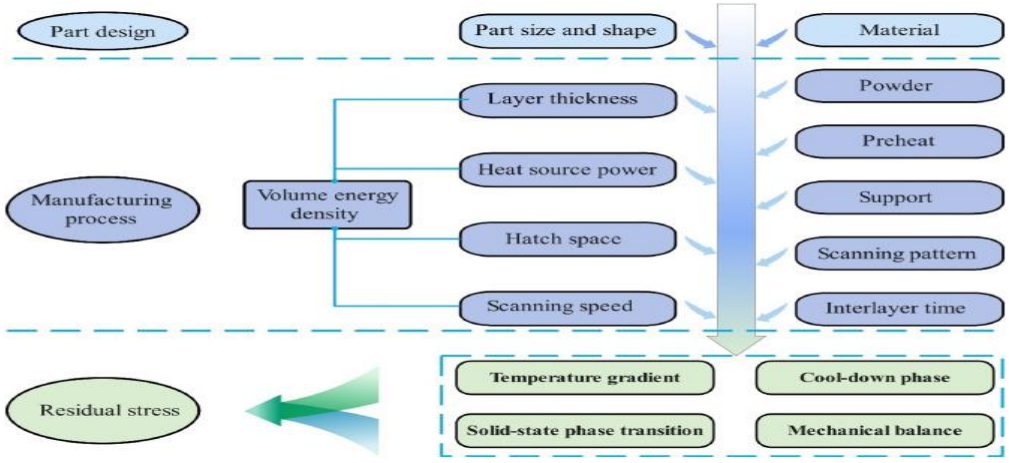

Fig 2.1: Process parameter dependencies of residual stress in AM [23].

2.2 Measurement of Residual Stress

There are two primary types of residual stress assessments based on whether the sample is destroyed: destructive methods and non-destructive methods. Destructive measurement techniques work on the basis of destroying a portion of the sample to break down the object's internal stress balance state and cause residual stress redistribution. The strain in the process is then measured and used to determine the residual stress using generalized Hooke's Law. Destructive measurement techniques that are frequently employed include the peeling, curvature, contour, and small hole procedures. Physical measuring techniques, also referred to as non-destructive residual stress measurement techniques, include magnetic techniques, ultrasonic waves, and X-ray and neutron diffraction. Thus, whether or not there is a unique link between the residual stress and the measured physical attribute, as well as the precision of the quantitative relationship, determine how accurate this method is. Furthermore, it should be noted that various residual stress measurement techniques have varying specifications for the sample's shape, composition, and surface condition. They also differ in terms of the appropriate measurement scale range, penetration depth, error, time, and cost. The figure displays the depth and resolution of a few popular techniques for measuring residual stress [23].

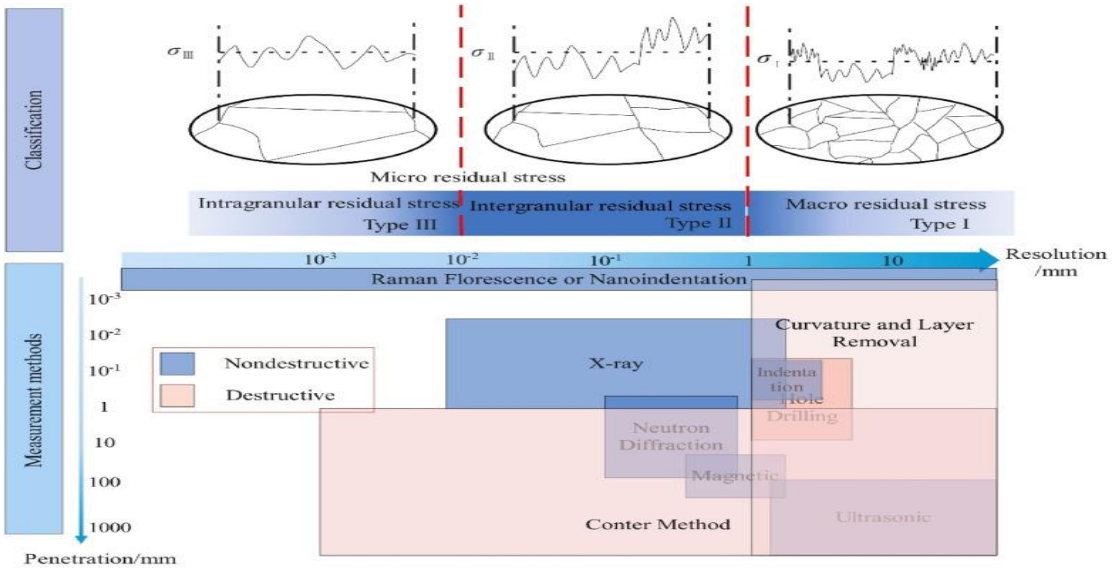

Fig 2.2: Classification and measurement method of residual stress [23]

CHAPTER 3
FORMULATION

3.1 Heat source model

In laser metal deposition (LMD), heat source models are essential for modeling residual stresses, microstructure evolution, and thermal behavior. Double ellipsoid and Gaussian models of heat sources are frequently employed in this procedure. In order to better describe complicated thermal behaviors in laser processes, these models approximate the distribution of thermal energy during deposition. The Goldak double-ellipsoid model provides an asymmetric distribution, while the Gaussian model represents a symmetric heat distribution. In simulations when it is assumed that the heat input spreads symmetrically around the laser beam, for example, the Gaussian heat source model is frequently used. A more realistic modeling of the heat distribution inside the melt pool is made possible by the Goldak model, which separates the heat source into two ellipsoids (front and rear) for both single-track and multi-track deposition situations. Because it can replicate the effects of temperature gradients that induce thermal expansion and contraction—which are directly related to stress and distortion in the material—this model is very helpful for predicting residual stresses [25].

When the energy distribution of the laser beam is radially symmetric, the Gaussian model is especially useful because it requires fewer parameters and requires less computational complexity than the Goldak model. This symmetry enables the Gaussian model to effectively capture the primary thermal behavior in the melt pool, especially in situations where fine asymmetry in heat distribution is less critical to the study's objectives. Therefore, using a Gaussian heat source model instead of the Goldak (double ellipsoid) model for laser metal deposition provides a simpler and frequently accurate method for simulating the symmetrical distribution of heat typical of many laser processes [26].

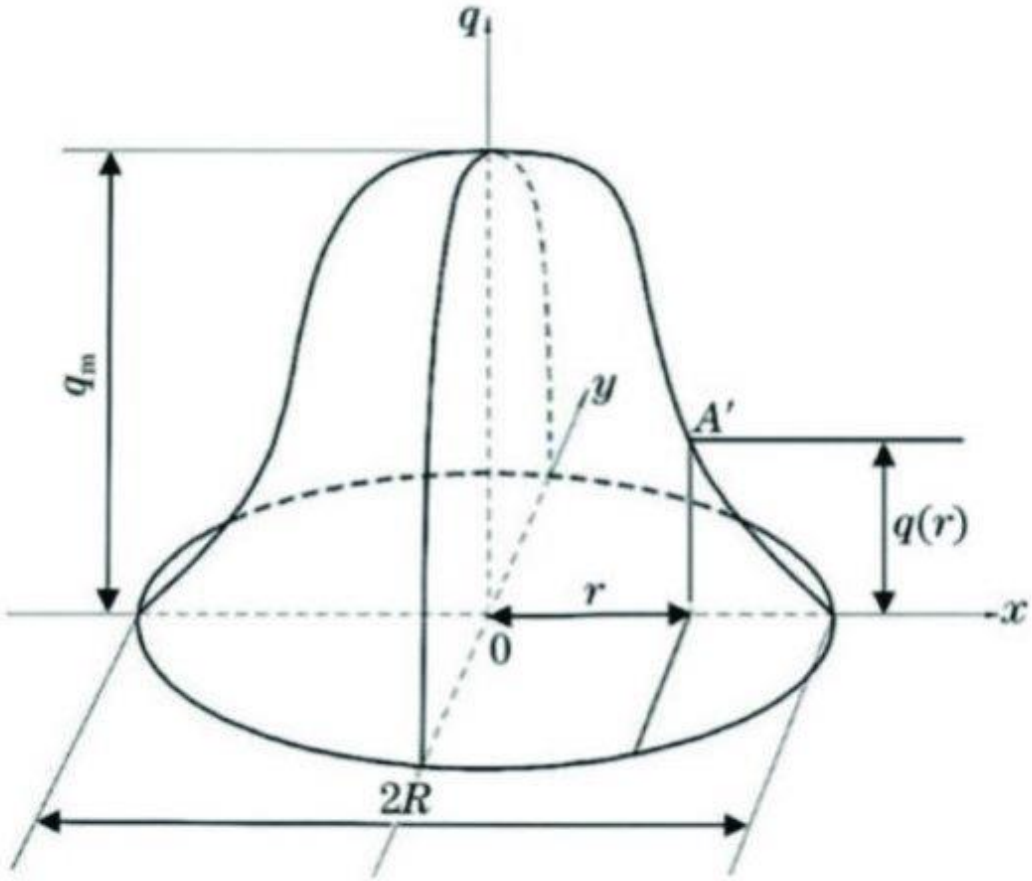

Fig 3.1: A Gaussian heat source model [27]

On the other hand, the Goldak model adds more parameters to model asymmetrical heat distributions, which makes it more appropriate for uses like arc welding, where the melt pool and solidification can be greatly impacted by such asymmetry. This extra complexity might not be required for laser metal deposition, though, as a Gaussian energy distribution can accurately depict the heat input from the beam without requiring extra computing power. For anticipating temperature profiles and residual stresses without making the simulation too complicated, the Gaussian model strikes a balance between modeling accuracy and computational economy [25].

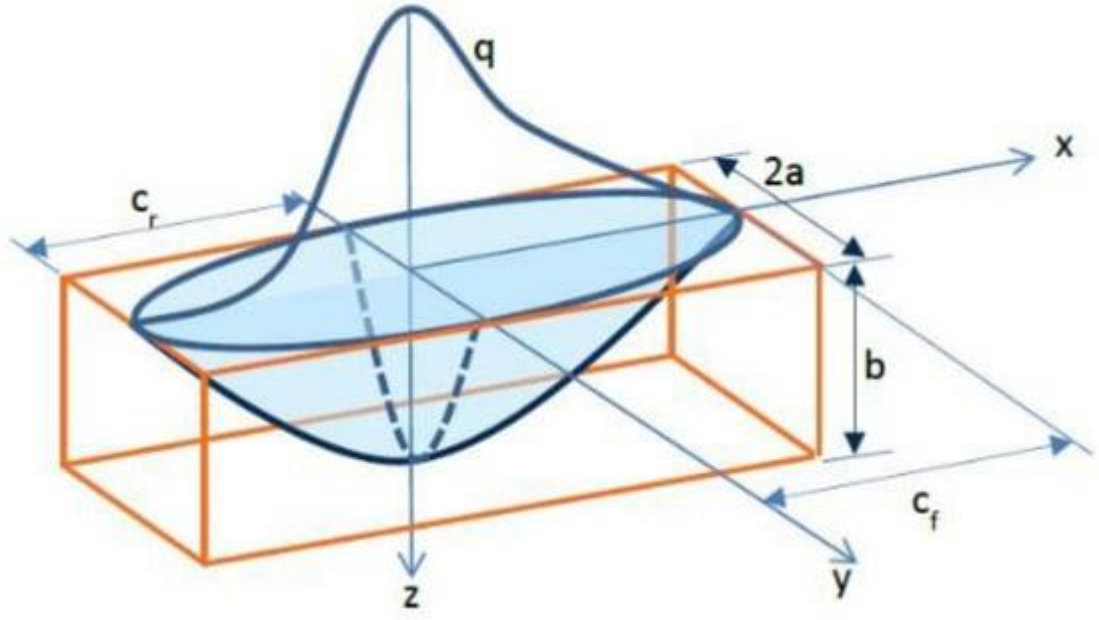

Fig 3.2: A Goldak heat source model [25]

3.2 Gaussian Heat Source Model

The volumetric heat source model mainly includes the Gaussian and double ellipsoid types. The heat flux in a Gaussian heat source model follows the Gaussian distribution.

The Gaussian heat source model typically defines the heat flux q(r) as:

$$q(r) = \frac{P}{\pi r_0^2} \, exp\left(-\frac{r^2}{r_0^2}\right) \quad \text{.....(3.1)}$$

where:

- P is the total power of the laser,
- r is the radial distance from the center of the beam,
- r_0 is the effective radius of the beam (defining where the intensity drops to 1/e of its peak value).

3.3 Volumetric heat distribution

For a three-dimensional Gaussian heat source, the distribution can extend vertically, which is useful for modeling how the laser penetrates the material. The volumetric heat flux q(x,y,z) can be expressed as:

$$q(x,y,z) = \frac{P}{\pi^{\frac{3}{2}} r_0^2 z_0} \, exp\left(-\frac{x^2+y^2}{r_0^2} - \frac{z^2}{z_0^2}\right) \quad \text{…….....(3.2)}$$

where:

- x, y, and z are spatial coordinates relative to the beam center,
- z_0 is the penetration depth parameter of the heat source.

When simulating materials with different absorption or situations where the laser does not evenly distribute heat vertically, this formula is helpful because it takes into account both the radial spread and the depth of the laser's penetration. The depth parameter z_0 gives you control over how deeply the heat penetrates.

3.4 Temperature Distribution Over Time (Heat Equation)

The transient heat conduction in the material due to the Gaussian heat source can be modelled by the heat equation**:**

$$\frac{\partial T}{\partial t} = \alpha \nabla^2 T + \frac{q(x,y,z)}{\rho c} \quad \text{.....(3.3)}$$

where:

- T is the temperature,
- t is time,
- α is the thermal diffusivity of the material,
- $\nabla^2 T$ is the Laplacian of temperature (captures heat diffusion),
- ρ is the material density,
- c is the specific heat capacity.

This partial differential equation (PDE) describes how heat is conducted over time within the material, combining conductive heat transfer and the applied heat flux from the laser. The term q(x,y,z)/(ρc) incorporates the Gaussian heat source, accounting for the heat input from the laser. Solving this equation provides a

transient temperature profile, allowing you to track temperature changes at different points over time.

3.5 Residual Stress from Thermal Gradient

Even though determining the residual stress from the Gaussian heat source is difficult and frequently calls for finite element analysis (FEA), thermal stress can be described simply as follows:

$$\sigma = E\alpha_t \Delta T \quad \text{.....(3.4)}$$

where:

- σ is the thermal stress,
- E is the Young's modulus,
- αt is the thermal expansion coefficient,
- ΔT is the temperature difference induced by the Gaussian heat source.

The stress produced by the temperature gradients from the Gaussian heat source can be estimated with the help of this equation. Thermal expansion and contraction caused by the laser's heating and cooling of various material regions produce stress, which might lead to residual stress if it is not uniform. Before doing in-depth FEA simulations, this basic model is sometimes used as an initial approximation. These formulas, which each handle a distinct aspect—heat distribution (radial and volumetric), temperature variation over time, and the possibility of residual stress generation—form the basis of Gaussian heat source modeling in laser metal deposition.

CHAPTER 4
METHODOLOGY

4.1 Objective

The initial phase of this study involved conducting an extensive literature review to understand the current state of knowledge regarding the Laser Metal Deposition (LMD) process and its effects on Stainless Steel 316 (SS 316). This review focused on identifying key findings from previous research that address the thermal behavior, microstructural changes, and mechanical properties associated with LMD of SS 316. Various scholarly articles, conference papers, and technical reports were analyzed to gather insights into the influence of process parameters—such as laser power, scan speed, and powder feed rate—on temperature distribution during deposition. The literature also highlighted the significance of temperature gradients in affecting solidification rates, phase transformations, and the development of residual stresses in the deposited material. This comprehensive review provided a theoretical foundation for the subsequent simulation phase and informed the selection of parameters for modeling the LMD process.

Key Findings: Simulation results show that thermal gradients

Residual Stress Identification: The study successfully identified the residual stresses in 316L material using FEA simulations in COMSOL, based on the laser heat source modeling.

Impact of Laser Parameters: The influence of various laser parameters (power, speed, and scan pattern) on the residual stress distribution was clearly observed.

Laser Heat Source Impact: The movement and parameters of the laser heat source determine the magnitude and distribution of residual stresses.

Optimization Potential: Optimizing LMD process parameters to minimize residual stresses, improving the performance and integrity of additive manufactured components.

Thermal-Mechanical Interactions: The thermal gradients and the mechanical responses due to the laser's heat input were the primary drivers for the observed residual stresses.

4.2 Simulation on COMSOL

The second phase, which came after the literature research, involves utilizing COMSOL Multiphysics to simulate the temperature distribution during the LMD process. A comprehensive model of dimension 25mm*10mm was built during this stage to simulate the thermal dynamics unique to SS 316 deposition. A scan speed of 5 mm/s, a beam diameter of 2 mm, and beginning and ambient temperature conditions set at 25 °C were among the important characteristics that were established. In order to represent realistic thermal interactions, suitable boundary conditions were constructed and the workpiece's geometry was precisely modeled. A thorough examination of the ensuing temperature distribution was made possible by the heat transfer model's incorporation of both convection to the external environment and conduction within the SS 316 material. Temperature profiles were produced after the simulation was run in order to evaluate crucial areas including the melt pool and the heat-affected zone (HAZ). Understanding how temperature gradients affect material behavior—especially with regard to solidification and the possibility of residual stresses—requires this analysis. In the end, our methodology integrates sophisticated thermal simulations with a comprehensive literature analysis to improve comprehension of LMD processes and guide tactics for material property optimization in additive manufacturing applications.

Average laser power density in Gaussian distribution, (W/m^2)

$$P_g = A\left[\frac{E_p}{P_w \frac{\pi}{4} d^2}\right] exp\left[-\frac{(x - x_r)^2}{2\emptyset^2}\right]$$

4.3 Experimental Validation

X-ray diffraction (XRD) will be used as a crucial experimental technique to verify the simulation results of temperature distribution and residual stresses in Stainless Steel 316 (SS 316) and Titanium Alloy Ti6Al4V (Ti-6-4). To ensure that the process parameters, such as laser power, scanning speed, and feed rate, are similar with those utilized in the simulations, samples of both materials will first undergo the Laser Metal Deposition (LMD) process to create a number of test specimens. The specimens will be surface prepared after deposition to get rid of any impurities or oxides that could affect the XRD analysis. A typical X-ray diffractometer will be used for the XRD measurements, and the samples will be positioned to optimize the detection of diffracted X-rays. The crystallographic structure and phase composition of the deposited materials may be determined by examining the diffraction patterns that arise. In particular, residual stresses will be ascertained by applying the $\sin^2\psi$ method [28], which connects the material's strain to the diffraction angle, and using the peak positions and broadening in the diffraction patterns. To confirm that the temperature distribution and stress predictions are accurate, the data from the XRD analysis will be compared with the simulated results. Additionally, any differences between the simulation and experimental data will be examined in order to improve the simulation model's predictive power for upcoming research on LMD processes and how they affect material properties.

$$\sigma = \frac{E}{1+\nu} * \frac{d * d_0}{d_0 \sin^2(\psi)} \quad \text{.....(4.1)}$$

- σ is the residual stress in the material.
- E is the Young's modulus of the material.
- ν is the Poisson's ratio of the material.
- d is the interplanar spacing of the diffracted plane measured at angle ψ
- d_0 is the interplanar spacing in the absence of residual stress (determined from the unstrained state).

- ψ is the angle between the incident X-ray beam and the normal to the surface of the sample (the tilt angle).

CHAPTER 5
NUMERICAL MODEL

For the temperature distribution simulation, COMSOL Multiphysics 6.2 is used. To begin simulating a moving heat source on a metal surface in COMSOL using a 2D setup, launch COMSOL and make a new 2D model. To precisely describe the thermal behavior, choose "Heat Transfer in Solids" as the main physics module in the describe Wizard. To take the mobility of the heat source over time into consideration, select a time-dependent study design. After choosing the study, proceed to the Geometry section to determine the workpiece geometry. The workpiece should be represented in 2D as a rectangle with the height and length adjusted to correspond with the dimensions of the plate that your experiment or theory is modeling.

After that, assign material qualities to the workpiece by going to the Materials section. If necessary, manually enter particular data or choose the relevant material from COMSOL's library, such as SS 316. Realistic temperature simulation requires precise thermal characteristics, such as density, specific heat capacity, and thermal conductivity were used from the data available, also the temperature and time dependent equations used.

To represent the laser or moving heat source, add a Heat Source node to the Heat Transfer in Solids interface. To replicate the focused energy distribution of a laser beam, set up the heat source with a Gaussian profile. Adjust the beam width and power based on the intended or experimental parameters. Define a time-dependent function to adjust the heat source's position across the 2D surface over time because it is moving. This can be accomplished by simulating the heat source's continuous movement in the x- or y-direction by adding a parametric expression.

Once the moving heat source has been defined, establish the beginning and boundary conditions. Usually, room temperature is used as the starting temperature. Provide boundary conditions, such as convective cooling at the margins if necessary, to replicate

real-world cooling. This facilitates the realistic replication of the heat dissipation behavior.

To capture fine-grained temperature gradients, mesh the geometry with a finer mesh in areas close to the heat source and a coarser mesh farther away. To see the heat distribution as the source moves across the 2D surface, solve the model after the mesh has been set up. To properly examine the heat flow and thermal gradients, observe the temperature distribution when the simulation is finished. To investigate stress patterns brought on by thermal expansion and cooling, add the Solid Mechanics module after the thermal solution if residual stress analysis is necessary. An effective and thorough perspective of the workpiece's reaction to the moving heat source is provided by this 2D model.

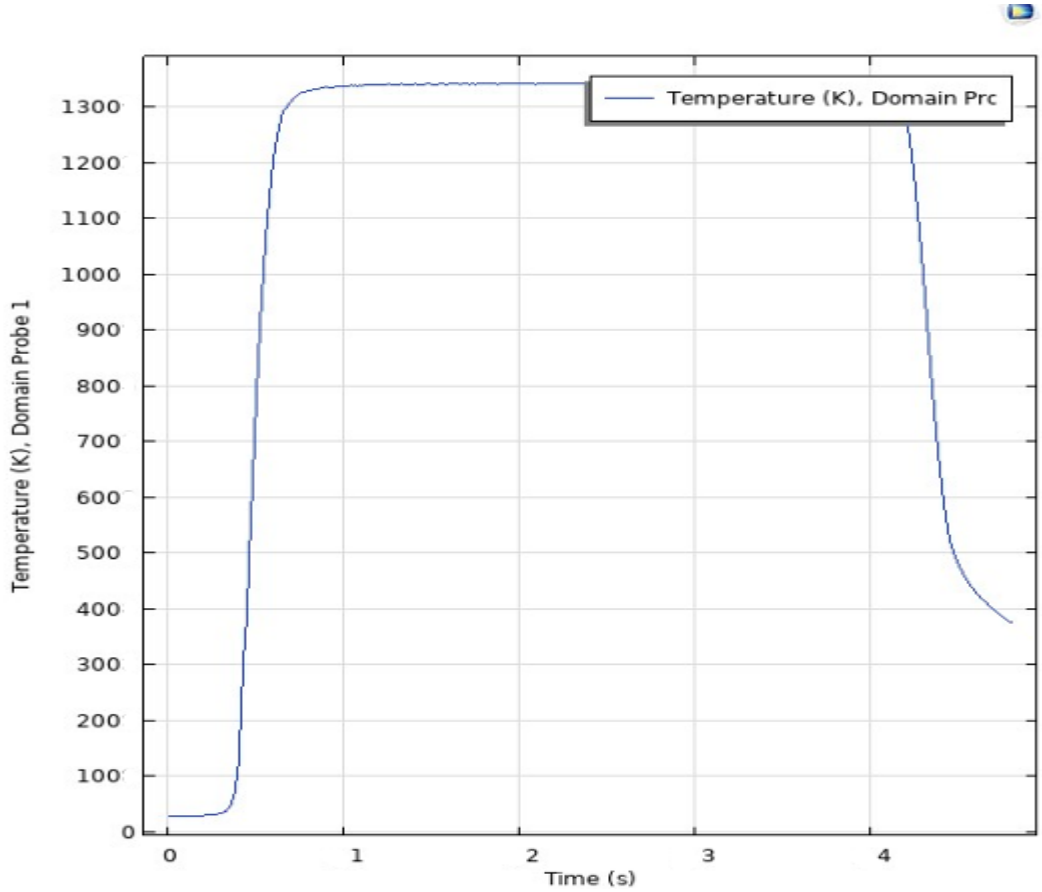

Fig 5.1: Temperature Vs Time plot

Laser Metal Deposition (LMD) Temperature Distribution Results for Stainless Steel 316

Simulation Setup:

- Material: Stainless Steel 316
- Laser Power: 300 W
- Scan Speed: 5 mm/s
- Beam Diameter: 2.5 mm
- Ambient Temperature: 293.15 K
- Initial Workpiece Temperature: 293.15 K
- Simulation Duration: 5 seconds

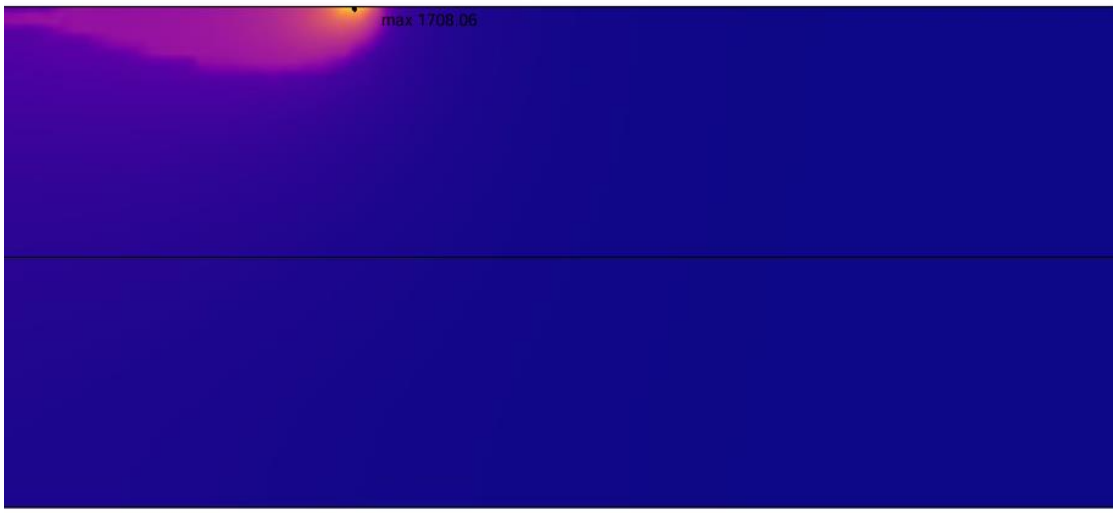

Fig 5.2: COMSOL Laser Beam Simulation

Average laser power density in Gaussian distribution, (W/m^2)

$$P_g = A\left[\frac{E_p}{P_w \frac{\pi}{4} d^2}\right] exp\left[-\frac{(x - x_r)^2}{2\emptyset^2}\right]$$

Evaluating the material's residual stresses is a crucial next step after collecting the temperature distribution from your simulation. Temperature variations encountered during the Laser Metal Deposition (LMD) process result in residual strains, which can cause differential expansion and contraction when the material cools. The ensuing stress

field within the workpiece can be modeled using Finite Element Analysis (FEA) and the temperature distribution data. For the purpose of forecasting probable failure spots, warping, or cracking during or after the deposition process, this study assists in locating areas of high tensile or compressive stresses. It is crucial to comprehend these residual pressures in order to guarantee the final part's integrity and dependability, particularly in important applications.

To ensure accuracy and dependability, it is essential to validate the simulation results using experimental techniques. This entails carrying out a number of tests to gauge the deposited material's hardness, microstructural characteristics, and residual stresses. It is possible to directly evaluate residual stress profiles using methods like neutron or X-ray diffraction. Hardness tests and metallographic analyses (such as optical or scanning electron microscopy) also reveal information on the material's microstructure, which can be compared to the simulation's expected attributes. The LMD process and its impacts on material characteristics can be better understood overall by comparing simulation results with experimental data. This allows you to fine-tune your model parameters for improved predictive capabilities in subsequent simulations.

REFERENCES

[1] "ISO/TC 261". "ISO/ASTM *52900 Additive manufacturing — General principles — Terminology*". (accessed: 22.09.2020).

[2] P.N. Sibisi, A.P.I. Popoola, N.K.K. Arthur, S.L. Pityana, Review on direct metal laser deposition manufacturing technology for the ti-6Al-4V alloy, Int. J. Adv. Manuf. Technol. 107 (2020) 1163–1178, https://doi.org/10.1007/s00170-019-04851-3

[3] Pellizzari, M., Zhao, Z., Bosetti, P., & Perini, M. (2022). Optimizing direct laser metal deposition of H13 cladding on CuBe alloy substrate. *Surface and Coatings Technology*, *432*, 128084. https://doi.org/10.1016/j.surfcoat.2022.128084

[4] Hu, Y., & Cong, W. (2018). A review on laser deposition-additive manufacturing of ceramics and ceramic reinforced metal matrix composites. *Ceramics International*, *44*(17), 20599-20612. https://doi.org/10.1016/j.ceramint.2018.08.083

[5] TRUMPF Inc. https://www.trumpf.com/en_US/solutions/applications/additive-manufacturing/laser-metal-deposition/

[6] Herzog, D., Seyda, V., Wycisk, E., & Emmelmann, C. (2016). Additive manufacturing of metals. *Acta Materialia*, *117*, 371-392. https://doi.org/10.1016/j.actamat.2016.07.019

[7] M. Yan and P. Yu, 'An Overview of Densification, Microstructure and Mechanical Property of Additively Manufactured Ti-6Al-4V — Comparison among Selective Laser Melting, Electron Beam Melting, Laser Metal Deposition and Selective Laser Sintering, and with Conventional Powder', Sintering Techniques of Materials. InTech, Apr. 01, 2015. doi: 10.5772/59275.

[8] Frazier, W.E. Metal Additive Manufacturing: A Review. *J. of Materi Eng and Perform* **23**, 1917–1928 (2014). https://doi.org/10.1007/s11665-014-0958-z

[9] Abdulrahman, K. O., Akinlabi, E. T., & Mahamood, R. M. (2017). Laser metal deposition technique: Sustainability and environmental impact. *Procedia Manufacturing*, *21*, 109-116. https://doi.org/10.1016/j.promfg.2018.02.100

[10] L. Xue, M. U. Islam, and A. Theriault, "Laser Consolidation Process for the Manufacturing of Structural Components for Advanced Robotic Mechatronic System – A State of Art Review," in *6th International Symposium on Artificial Intelligence and Robotics & Automation in Space*, 2001.

[11] Laser. (2024, November 1). In *Wikipedia*. https://en.wikipedia.org/wiki/Laser

[12] D. Paschotta, "Lasers",: https://www.rp-photonics.com/lasers.html.

[13] M. Alves, "Tecnologias Laser", Leiria, 2018

[14] Rami Arieli: "The Laser Adventure" Section 6.2.1 page 4

[15] D. Belforte**,** "The three phases of lasers: solid state, gas, and liquid," *Laser Focus World*, Feb. 1, 2008. Available: https://www.laserfocusworld.com/lasers-sources/article/16553578/the-three-phases-of-lasers-solid-state-gas-and-liquid

[16] I. Garmendia, J. Leunda, J. Pujana and A. Lamikiz, "In-process height control during laser metal deposition based on structured light 3D scanning", Procedia CIRP, vol. 68, pp. 375-380, 2018.
[17] Ghasempour-Mouziraji, M., Lagarinhos, J., Afonso, D., & Alves de Sousa, R. (2024). A review study on metal powder materials and processing parameters in Laser Metal Deposition. *Optics & Laser Technology*, *170*, 110226. https://doi.org/10.1016/j.optlastec.2023.110226
[18] Gharbi, M., Peyre, P., Gorny, C., Carin, M., Morville, S., Le Masson, P., Carron, D., & Fabbro, R. (2013). Influence of various process conditions on surface finishes induced by the direct metal deposition laser technique on a Ti–6Al–4V alloy. *Journal of Materials Processing Technology*, *213*(5), 791-800. https://doi.org/10.1016/j.jmatprotec.2012.11.015
[19] Amine, T., Newkirk, J. W., & Liou, F. (2014). Investigation of effect of process parameters on multilayer builds by direct metal deposition. *Applied Thermal Engineering*, *73*(1), 500-511. https://doi.org/10.1016/j.applthermaleng.2014.08.005
[20] Tan, H., Shang, W., Zhang, F., Clare, A. T., Lin, X., Chen, J., & Huang, W. (2018). Process mechanisms based on powder flow spatial distribution in direct metal deposition. *Journal of Materials Processing Technology*, *254*, 361-372. https://doi.org/10.1016/j.jmatprotec.2017.11.026
[21] “Plasma Atomization（PA）_Avimetal Powder Metallurgy Technology Co,.Ltd.” [Online].
[22] Matweb Material Property Data, [Online], https://www.matweb.com/search/DataSheet.aspx?MatGUID=dfced4f11d63459e8ef8733d1c7c1ad2
[23] Chen, S., Gao, H., Zhang, Y., Wu, Q., Gao, Z., & Zhou, X. (2022). Review on residual stresses in metal additive manufacturing: Formation mechanisms, parameter dependencies, prediction and control approaches. *Journal of Materials Research and Technology*, *17*, 2950-2974. https://doi.org/10.1016/j.jmrt.2022.02.054
[24] Kenel, C., Grolimund, D., Li, X., Panepucci, E., Samson, V. A., Sanchez, D. F., Marone, F., & Leinenbach, C. (2017). In situ investigation of phase transformations in Ti-6Al-4V under additive manufacturing conditions combining laser melting and high-speed micro-X-ray diffraction. *Scientific Reports*, *7*(1), 1-10. https://doi.org/10.1038/s41598-017-16760-0
[25] Kiran, A., Li, Y., Hodek, J., Brázda, M., Urbánek, M., & Džugan, J. (2021). Heat Source Modeling and Residual Stress Analysis for Metal Directed Energy Deposition Additive Manufacturing. *Materials*, *15*(7), 2545. https://doi.org/10.3390/ma15072545
[26] Zhang, Z., Wang, Y., Ge, P., & Wu, T. (2022). A Review on Modelling and Simulation of Laser Additive Manufacturing: Heat Transfer, Microstructure Evolutions and Mechanical Properties. *Coatings*, *12*(9), 1277. https://doi.org/10.3390/coatings12091277
[27] Wang, J., Zhang, Q., Shen, W., Liang, Z., Chang, C., Yang, L., Li, J., & Huang, F. (2022). Failure Analysis of Chromium Plating Layer on a Piston Rod Surface and the Study of Ni-Based Composite Coating with Nb Addition by Laser Cladding. *Metals*, *12*(7), 1194.https://doi.org/10.3390/met12071194
[28] Fitzpatrick, M.E.; Fry, A.T.; Holdway, P.; Kandil, F.A.; Shackleton, J.; Suominen, L. Determination of residual stresses by X-ray diffraction. Meas. Good Pract. Guide 2005

[29] Vora, H. D., & Dahotre, N. B. (2015). Surface topography in three-dimensional laser machining of structural alumina. *Journal of Manufacturing Processes*, *19*, 49-58. https://doi.org/10.1016/j.jmapro.2015.04.002